

Supporting Information

Mononuclear Fe(III) complexes with 2,4-dichloro-6-((quinoline-8-ylimino)methyl)phenolate: synthesis, structure, and magnetic behavior

Ah Rim Jeong,^a Si Ra Park,^b Jong Won Shin,^{*,a} Jihyun Kim,^b Ryuya Tokunaga,^c Shinya Hayami^c and Kil Sik Min^{*,b}

^a Department of Chemistry, Kyungpook National University, Daegu 41566, Republic of Korea

^b Department of Chemistry Education, Kyungpook National University, Daegu 41566, Republic of Korea

^c Department of Chemistry, Kumamoto University, Kumamoto 860-8555, Japan

E-mail: jwshin@kisti.re.kr (J. W. S.); minks@knu.ac.kr (K. S. M.)

Table S1 Summary of crystallographic data for **1a–3b**

	1a	1b	2a	2b	3a	3b
formula	C ₃₂ H ₂₀ Cl ₄ Fe N ₅ O ₆	C ₃₂ H ₂₀ Cl ₄ Fe N ₅ O ₆	C ₃₈ H ₃₀ B ₂ Cl ₄ F 4FeN ₄ O ₄	C ₃₂ H ₁₈ B ₂ Cl ₄ F 4FeN ₄ O ₂	C ₃₂ H ₁₈ Cl ₅ Fe N ₄ O ₆	C ₃₂ H ₁₈ Cl ₅ Fe N ₄ O ₆
M _r	768.18	768.18	891.12	774.96	787.60	787.60
crystal system	Triclinic	Triclinic	Triclinic	Triclinic	Monoclinic	Monoclinic
space group	P $\bar{1}$	P $\bar{1}$	P $\bar{1}$	P $\bar{1}$	P2 ₁ /c	P2 ₁ /c
a (Å)	9.4930(19)	9.5590(19)	9.4580(19)	9.5750(19)	14.227(3)	14.289(3)
b (Å)	11.327(2)	11.905(2)	12.391(3)	12.544(3)	17.461(4)	17.702(4)
c (Å)	15.069(3)	15.101(3)	16.320(3)	16.518(3)	15.213(3)	15.399(3)
α (deg)	105.08(3)	108.20(3)	95.32(3)	94.12(3)	90	90
β (deg)	100.34(3)	98.16(3)	103.38(3)	103.45(3)	107.55(3)	107.82(3)
γ (deg)	94.92(3)	96.48(3)	97.00(3)	97.39(3)	90	90
V (Å ³)	1524.1(6)	1593.2(6)	1832.3(7)	1902.8(7)	3603.2(14)	3708.1(14)
Z	2	2	2	2	4	4
D _{calc} (g cm ⁻³)	1.674	1.601	1.615	1.353	1.485	1.443
T (K)	100(2)	298(2)	100(2)	298(2)	100(2)	293(2)
λ (Å)	0.70000	0.70000	0.63000	0.63000	0.63000	0.63000
μ (mm ⁻¹)	0.868	0.831	0.552	0.520	0.595	0.579
Reflections collected	14642	12123	28979	15631	37245	37942
Independent reflections	7484	6283	14908	9786	9566	9877
Reflections with > 2 σ (I)	5520	4194	8986	6035	8284	7465
R _{int}	0.0184	0.0238	0.0347	0.0478	0.0267	0.0435
Goodness-of-fit on F^2	1.041	0.983	1.083	1.500	1.031	1.047
R ₁ ^a (4 σ data)	0.0711	0.0611	0.0732	0.0967	0.0607	0.0748
wR ₂ ^b (4 σ data)	0.1912	0.1566	0.2274	0.2870	0.1557	0.2342
CCDC no.	2002656	2002657	2002658	2002659	2002660	2002661

^a R₁ = $\sum||F_o| - |F_c||/\sum|F_o|$. ^b wR₂ = [$\sum w(F_o^2 - F_c^2)^2 / \sum w(F_o^2)^2$]^{1/2}.

Table S2 Temperature-dependent μ_{eff} of **1** obtained by NMR spectra of Fig. S1

Molarity (M)	A (ppm)	B (ppm)	$\Delta\delta$ (ppm)	χ_M	T (K)	μ_{eff}
1.68×10^{-2}	8.324	8.096	0.228	3.23×10^{-3}	220	2.38
1.68×10^{-2}	8.337	8.087	0.250	3.55×10^{-3}	230	2.56
1.68×10^{-2}	8.355	8.077	0.278	3.96×10^{-3}	240	2.76
1.68×10^{-2}	8.381	8.067	0.314	4.46×10^{-3}	250	2.99
1.68×10^{-2}	8.514	8.031	0.483	6.88×10^{-3}	300	4.04
1.68×10^{-2}	8.016	7.582	0.434	6.29×10^{-3}	340	4.14
1.68×10^{-2}	8.160	7.744	0.416	6.03×10^{-3}	380	4.28

Table S3 Temperature-dependent μ_{eff} of **2** obtained by NMR spectra of Fig. S2

Molarity (M)	A (ppm)	B (ppm)	$\Delta\delta$ (ppm)	χ_M	T (K)	μ_{eff}
1.26×10^{-2}	8.326	8.095	0.231	4.36×10^{-3}	220	2.77
1.26×10^{-2}	8.361	8.074	0.287	5.41×10^{-3}	240	3.22
1.26×10^{-2}	8.420	8.056	0.364	6.87×10^{-3}	260	3.78
1.26×10^{-2}	8.483	8.040	0.443	8.36×10^{-3}	280	4.33
1.26×10^{-2}	8.517	8.030	0.487	9.18×10^{-3}	300	4.70
1.26×10^{-2}	8.530	8.021	0.508	9.58×10^{-3}	320	4.95
1.26×10^{-2}	8.528	8.014	0.514	9.70×10^{-3}	340	5.14
1.26×10^{-2}	8.523	8.008	0.515	9.71×10^{-3}	360	5.29
1.26×10^{-2}	8.504	8.004	0.500	9.43×10^{-3}	380	5.35

Table S4 Temperature-dependent μ_{eff} of **3** obtained by NMR spectra of Fig. S3

Molarity (M)	A (ppm)	B (ppm)	$\Delta\delta$ (ppm)	χ_M	T (K)	μ_{eff}
1.32×10^{-2}	8.319	8.096	0.223	4.03×10^{-3}	220	2.66
1.32×10^{-2}	8.352	8.072	0.280	5.05×10^{-3}	240	3.11
1.32×10^{-2}	8.402	8.057	0.345	6.23×10^{-3}	260	3.60
1.32×10^{-2}	8.466	8.039	0.427	7.71×10^{-3}	280	4.16
1.32×10^{-2}	8.495	8.030	0.465	8.40×10^{-3}	300	4.49
1.32×10^{-2}	8.507	8.022	0.485	8.76×10^{-3}	320	4.74
1.32×10^{-2}	8.505	8.014	0.491	8.88×10^{-3}	340	4.91
1.32×10^{-2}	8.495	8.008	0.487	8.80×10^{-3}	360	5.03
1.32×10^{-2}	8.479	8.005	0.474	8.56×10^{-3}	380	5.10

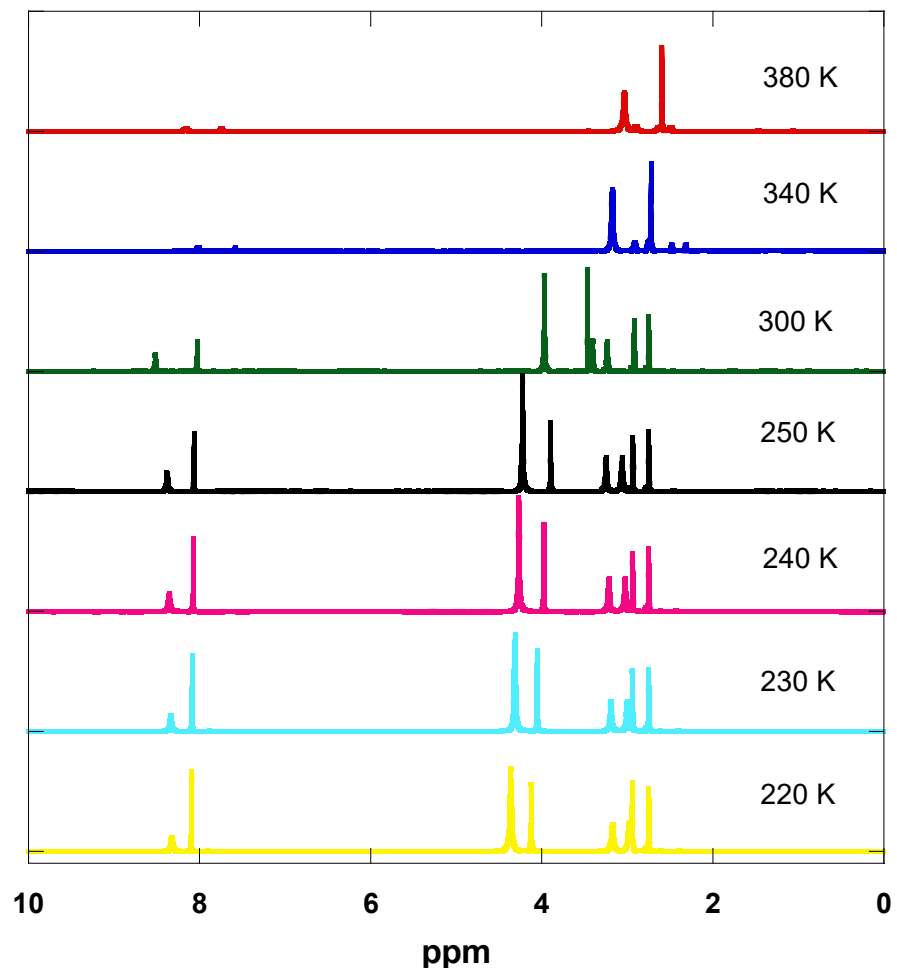


Fig. S1 Temperature-dependent NMR spectra of **1** measured by Evans method in DMF-d₇.

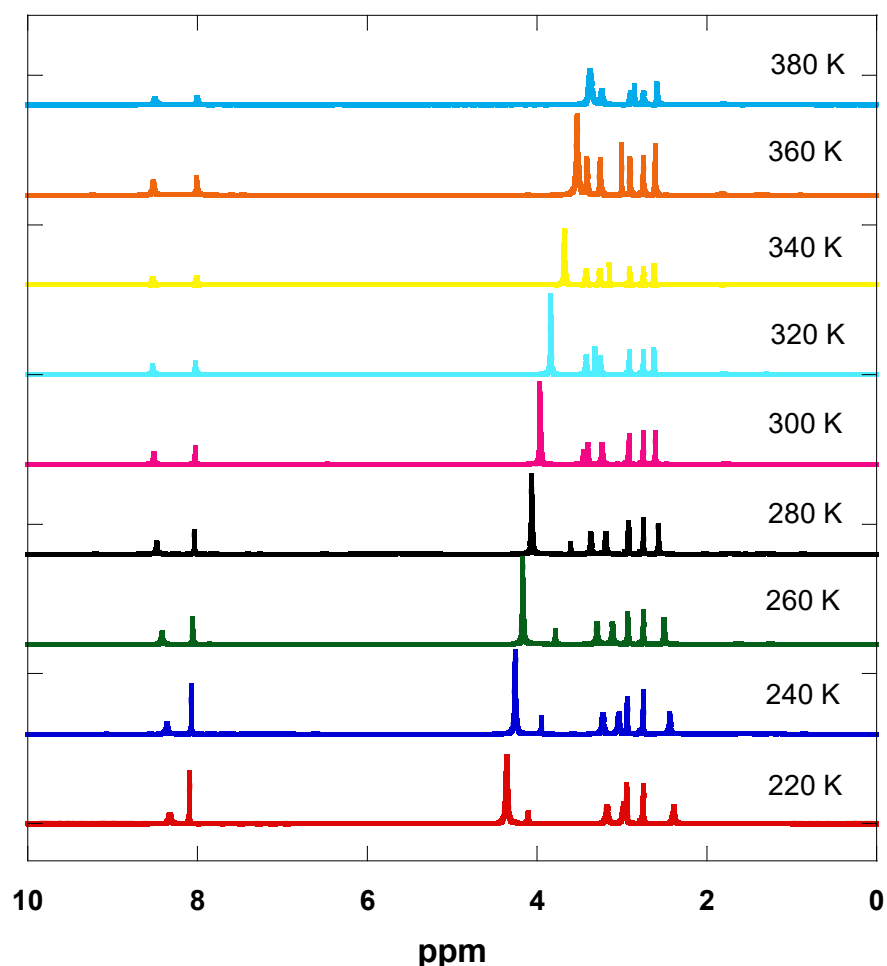


Fig. S2 Temperature-dependent NMR spectra of **2** measured by Evans method in DMF-d₇.

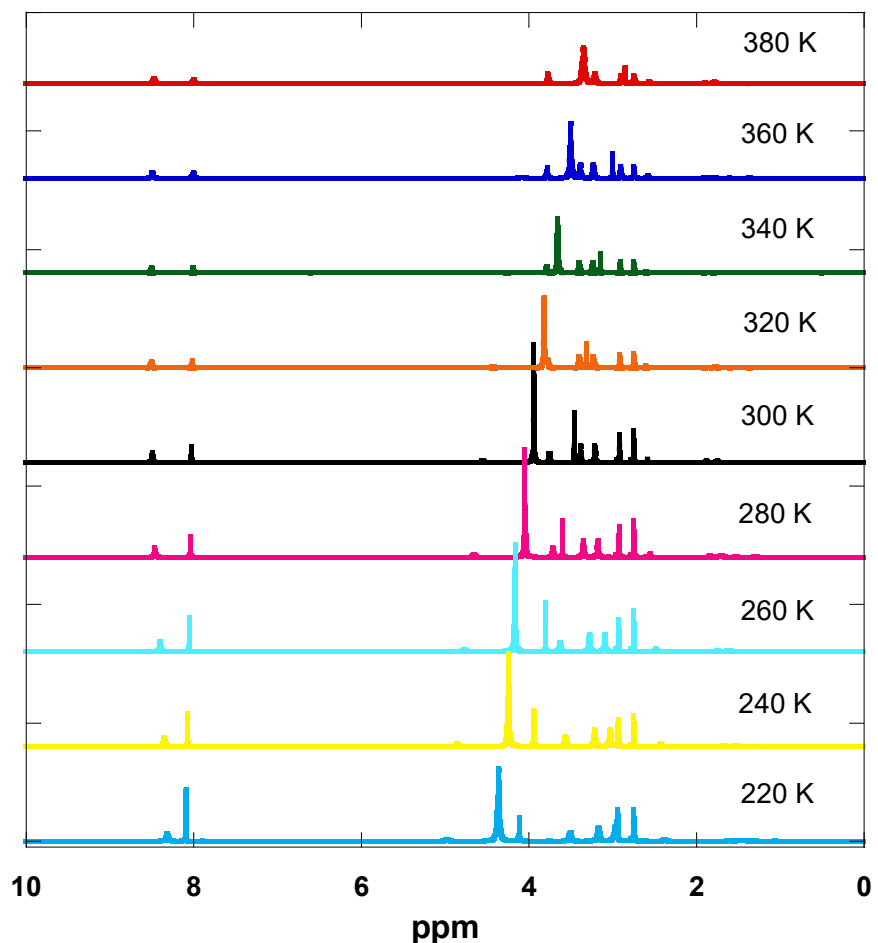


Fig. S3 Temperature-dependent NMR spectra of **3** measured by Evans method in DMF-d_7 .

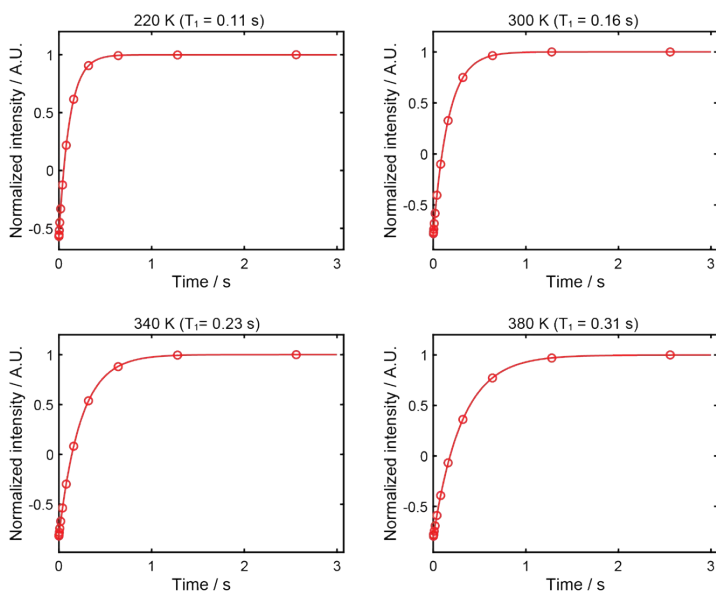


Fig. S4 ^1H T_1 relaxation curve fitting of DMF with **1** at 220, 300, 340, and 380 K.

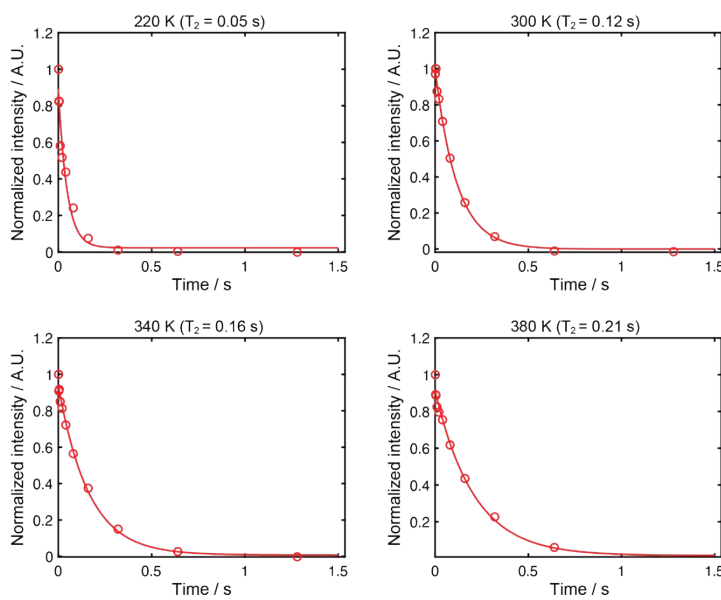


Fig. S5 ^1H T_2 relaxation curve fitting of DMF with **1** at 220, 300, 340, and 380 K.

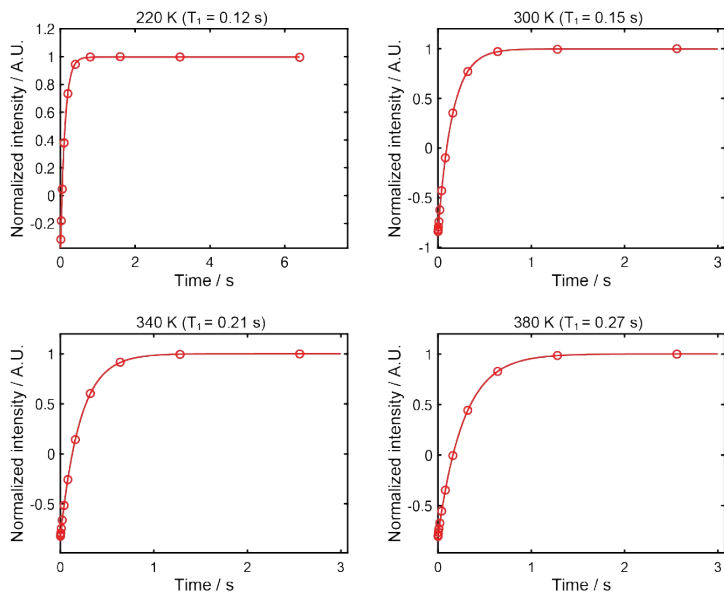


Fig. S6 ^1H T_1 relaxation curve fitting of DMF with **2** at 220, 300, 340, and 380 K.

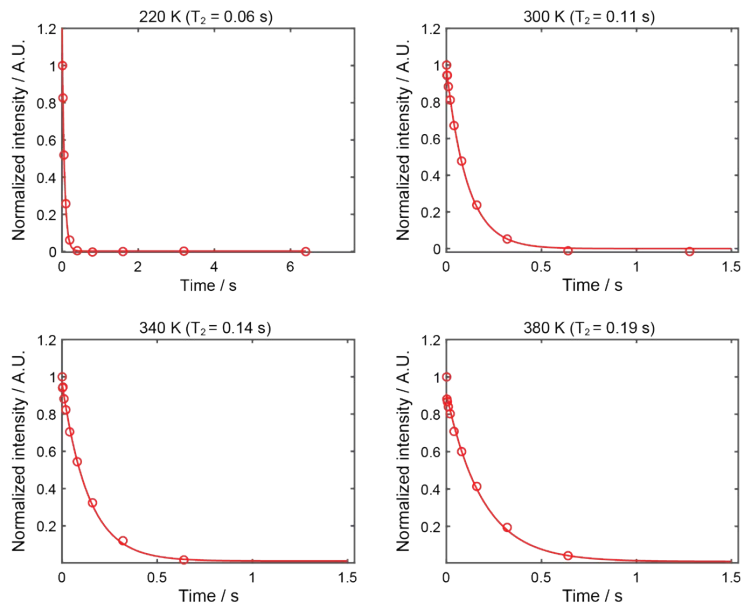


Fig. S7 ^1H T_2 relaxation curve fitting of DMF with **2** at 220, 300, 340, and 380 K.

Analyses of electron density map and F_{obs} vs F_{calc} plot of complexes **1a, **1b**, **2a**, **2b**, **3a**, and **3b**.**

Although the quality of the crystallographic data obtained may not be ideal (Figs S8~S13), but we are confident that the structural information derived is sufficient to support the conclusions presented in our manuscript. In particular, it is important to emphasize that the crystals available for complexes **1a**, **1b**, **2a**, **2b**, **3a**, and **3b** were not sufficient size, quality, or scattering strength for the laboratory diffractometer, so that satisfactory structures could only be collected using synchrotron radiation.

Specifically, the electron density maps of **1a**, **1b**, **2a**, **2b**, **3a**, and **3b** (Figs S8~S13) indicate some disorders in the anions, solvent areas, and high electron density of Cl atoms in the qsal-type ligand. Additionally, the F_{obs} vs. F_{calc} plots do not show narrow lines with numerous strong reflections, indicative of relatively poor agreements with the structural models (Figs S8~S13). This may also, in part, be attributed to the fact that single crystal data were acquired at a synchrotron beamline dedicated to small-molecule crystallography, which only permits a high-accuracy omega scan. This limitation could contribute to observed features in the F_{obs} vs. F_{calc} plots and completeness, particularly, for structures with low symmetry, tri-/monoclinic space group as here.

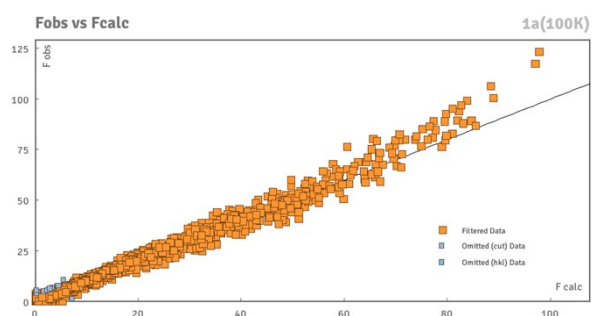
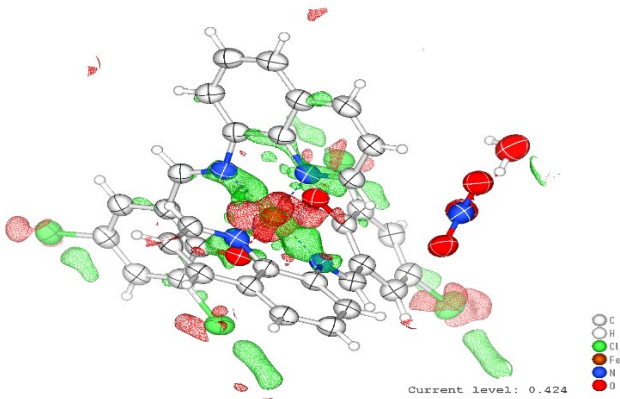


Fig. S8 Electron density map(up) and F_{obs} vs F_{calc} plot(down) of complex **1a**.

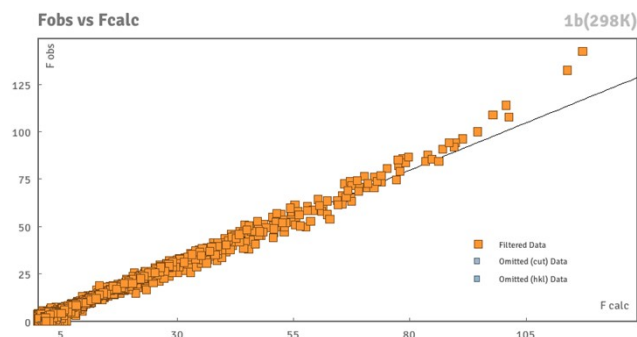
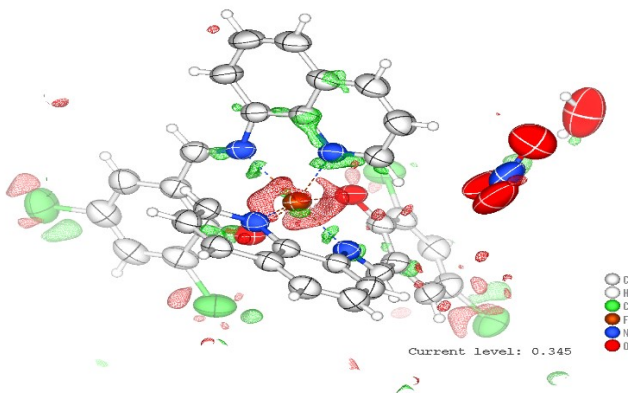


Fig. S9 Electron density map(up) and F_{obs} vs F_{calc} plot(down) of complex **1b**.

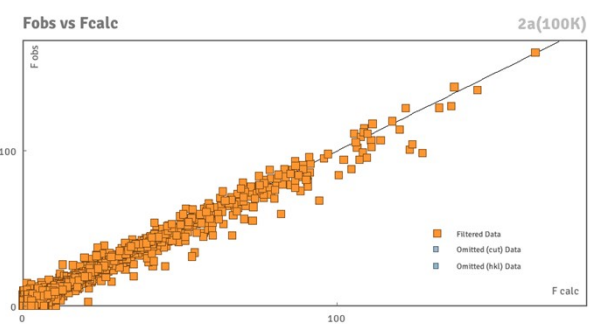
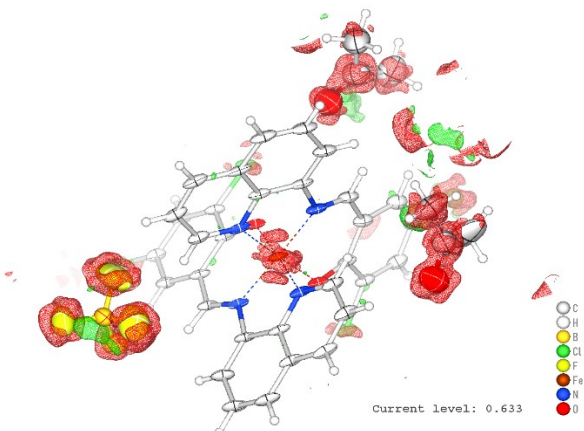


Fig. S10 Electron density map(up) and F_{obs} vs F_{calc} plot(down) of complex **2a**.

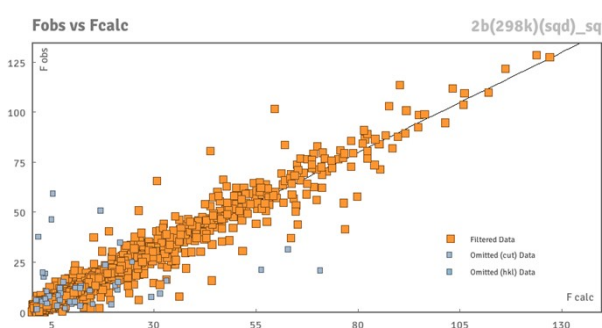
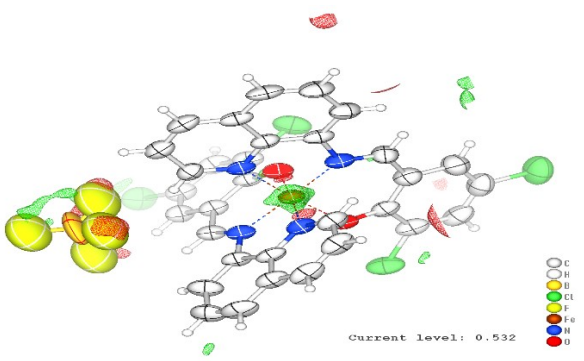


Fig. S11 Electron density map(up) and F_{obs} vs F_{calc} plot(down) of complex **2b**.

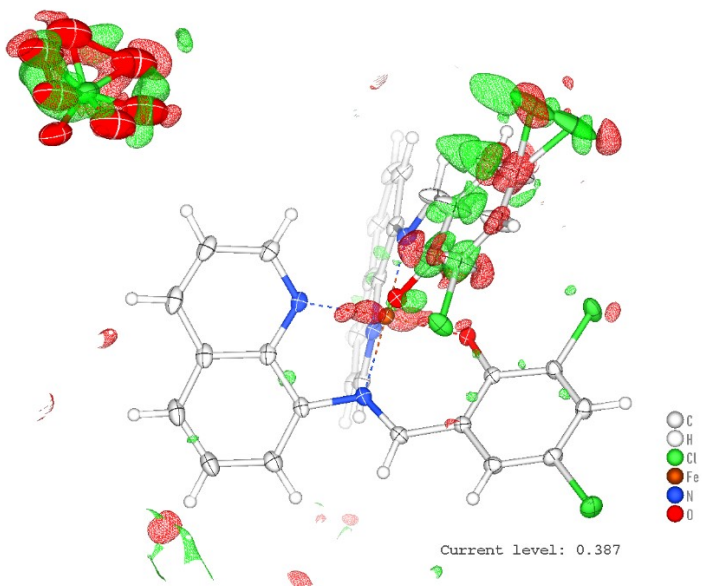


Fig. S12 Electron density map of **3a**.

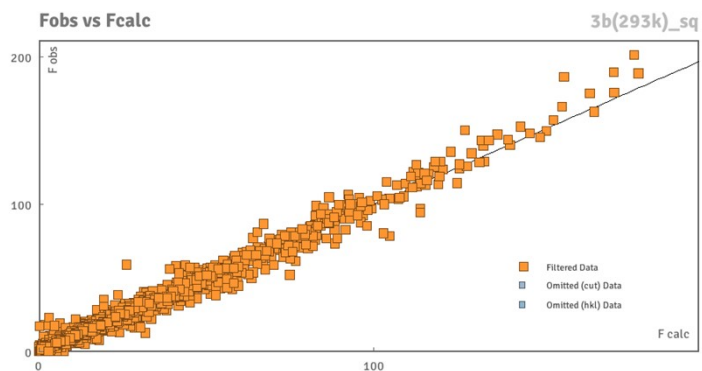


Fig. S13 F_{obs} vs F_{calc} plot of complex **3b**.